LAWRENCE
LIVERMORE
NATIONAL
LABORATORY

UCRL-JRNL-213433

Atomistic Modeling of Wave Propagation in Nanocrystals

E. Bringa, A. Caro, M. Victoria, N. Park

July 7, 2005

Journal of Metals

Disclaimer

This document was prepared as an account of work sponsored by an agency of the United States Government. Neither the United States Government nor the University of California nor any of their employees, makes any warranty, express or implied, or assumes any legal liability or responsibility for the accuracy, completeness, or usefulness of any information, apparatus, product, or process disclosed, or represents that its use would not infringe privately owned rights. Reference herein to any specific commercial product, process, or service by trade name, trademark, manufacturer, or otherwise, does not necessarily constitute or imply its endorsement, recommendation, or favoring by the United States Government or the University of California. The views and opinions of authors expressed herein do not necessarily state or reflect those of the United States Government or the University of California, and shall not be used for advertising or product endorsement purposes.

Atomistic Modeling of Wave Propagation in Nanocrystals

E.M. Bringa, A. Caro, M. Victoria

Lawrence Livermore National Laboratory, Livermore CA 94550, USA

N. Park

AWE, Aldermaston, Reading, Berkshire, RG7 4PR, UK

We present non-equilibrium molecular dynamics (MD) simulations of wave propagation in nanocrystals. We find that the width of the traveling wave front increases with grain size, d, as $d^{1/2}$. This width also decreases with the pressure behind the front. We extrapolate our results to micro-crystals and obtain reasonable agreement with experimental data. In addition, our extrapolation agrees with models that only take into account the various velocities of propagation along different crystalline orientations, without including grain boundary effects. Our results indicate that, even at the nanoscale, the role of grain boundaries as scattering centers or as sources of plasticity does not increase significantly the width of the traveling wave.

INTRODUCTION

Nanocrystals have been extensively studied, both in experiments[1] and simulations[2-4], for their numerous beneficial properties, for instance for their large strength. In general, continuum-scale plasticity models only include polycrystalline effects by averaging over various crystalline directions to obtain some "effective" isotropic material[5]. There are several models that do include full polycrystalline anisotropy, but where grain boundaries (GB) are considered infinitesimally thin, or not influencing the deformation of the material[6]. Few recent models have tried to incorporate the role of grain boundaries[7,8], but the connection to atomic-scale processes is only recently emerging[9].

Many current experiments[1] and most atomistic simulations on nanocrystals[2-4] involve homogeneous deformation of the material, i.e. the whole system is subjected to the same deformation. However, there may be instances, especially at very high strain rates, where this would be no longer true[10]; a wave will travel trough the material, with deformed material behind the wave front. Here we focus on how the nanocrystalline structure can change the wave propagation, due to polycrystalline effects. It is important to understand in detail the response of polycrystalline materials to wave propagation for a number of applications. For instance, the National Ignition Facility (NIF)[11] will require polycrystalline ignition targets where the wave front has to be extremely smooth to avoid Rayleigh-Taylor[12] instabilities caused by perturbations due to the grain structure. Such instabilities can grow resulting in a final compression diminished below the desired value.

There has been a large number of both experimental[13-16] and continuum modeling studies[10,17-23] on wave propagation in polycrystals, and samples with different grain size do show grain size dependence in wave propagation[13,16,18,21]. However, models that include atomic-level information are lacking. Fig. 1 shows a schematic of a wave traversing a polycrystal. In Fig. 1(a), the wave is crossing a single crystal, and the wave front is “straight”, since there are no perturbations (except for possible plasticity or phase transformations). A polycrystal introduces different wave velocities in each grain, with preferred wave propagation directions, as shown in Fig. 1(b). This fact alone would greatly enhance the wave front width, if the difference between propagation velocities is not negligible. For instance, for many fcc metals, the sound velocity along the “fast” direction, can be 10-25% larger than the velocity along the “slow” direction[17,18,24]. Some models do include the role of anisotropy leading to refraction of the wave, for instance, by increasing the effective path it travels[18]. In

addition to the polycrystal anisotropy, GB could play a role as scattering centers, or barriers to the wave transmission, with a fraction of the wave dissipated, as indicated in Fig. 1(c). Finally, Fig. 1(d) shows that GB can also act as sources of dislocations, where the plastic deformation may change the width of the wave front. There are several calculations[17,18,21] estimating the effect sketched in Fig. 1(b), but there are no analytical or semi-analytical models to predict shock width for a given grain size. Although there have been a few studies for single grain boundaries[25,26], there are no studies regarding the effects sketched in Figs. 1(c) and (d) in polycrystals. Following Fig. 1, the general expression of the width of the front, Δz, could be assumed to be the sum of (as a first approximation) independent contributions from Figs. 1(b)-(c):

$$\Delta z = \Delta z_{aniso} + \Delta z_{GBscatt} + \Delta z_{plastic} \qquad (1).$$

We can obtain an upper estimate of Δz_{aniso} from a 2D propagation case as follows. Imagine two rows of grains, one consisting only of grains where the velocity is "slow" and the other where the velocity is "fast". The spread Δz of the front after a time t will be $\Delta v\, t$, where Δv is the velocity differential. For a sample of fixed length L, with grains of size d, $L/d=N_g$ is the mean number of traversed grains, and $t=L/\langle v\rangle$. Therefore we can write:

$$\Delta z = (\Delta v/\langle v\rangle)\, d\, N_g = A_v\, d\, N_g, \qquad (2)$$

where we call $(\Delta v/\langle v\rangle) = A_v$ the "anisotropy factor". For a sample with many "rows", and grains of size d, with the same number of "slow" and "fast" grains randomly distributed, one would still expect a linear dependence of Δz with the anisotropy factor. However, there will be a large number of "rows" where the number of "slow" and "fast" grains will be roughly the same, giving $\Delta z_{aniso}\sim 0$. Assuming a power law form for the grain size dependence, d^{α}, this would give a dependence with $\alpha<1$. The fact that the shock width increases with grain size

has been experimentally observed for metals[13] and oxides[16]. Recent modeling[21] of this process for wave propagation in Be polycrystals gave $\alpha \sim 1/2$. Note that Eq. (2) also predicts that a wave will continue widening with time, or as it traverses more and more grains.

ATOMISTIC SIMULATIONS

Typical GBs in real materials are only ~1nm thick, and are difficult to model using continuum models. In this paper we use the massively parallel code MDCASK[27] to carry out atomistic molecular dynamics (MD) simulations of embedded atom method (EAM) copper samples[28]. Prismatic samples were built using the Voronoi construction with random texture[3]. Dislocation cores were identified using a centro-symmetry parameter filter[29]. We focus on the propagation of waves moving faster than the sound speed, i.e. shock waves. There are numerous MD simulations of shocks in single crystals[24,30-32], but only a limited number on polycrystalline materials[31-33]. We have simulated samples with 0.5-64 million atoms, and average grain sizes of 5, 10 and 20 nm on 32-768 CPUs. Further analysis of our simulation results is in progress and will be published elsewhere[33]. Our samples had free surfaces along the shock wave direction and periodic boundary conditions in the transverse direction. The first few surface layers on one side were chosen as a piston. A step velocity function was applied to these piston atoms at the desired piston velocity, U_p to create a traveling wave, with velocity U_s[24]. The stress along the shock direction (the shock pressure) behind the front is given by the Hugoniot equations[30] dealing with mass, momentum and energy conservation at the front: $P_H=\rho_0 U_p U_s$. The strain behind the front is constant and given by $\varepsilon=U_p/U_s$. Assuming a linear Hugoniot relationship, $U_s=c_0 + s_1 U_p$. For Cu, c_0=4.0 km/s, and s_1=1.5[24]. Our MD simulations[24] have shown that this equation is a reasonable approximation for this EAM potential, especially for strong shocks.

Fig. 2 shows snapshots of a simulation with d~5 nm and P=22 GPa (strain is ~10%). Despite the small grain size we observe significant dislocation activity, driven by the large applied stress. Partial dislocations are emitted from the GB and cross the grain leaving a stacking fault behind[33], as in previous homogeneous deformation simulations of larger grains[2,3]. Given the large level of plastic activity, one could expect large influences at the shock front for the simulated cases, as suggested in Fig. 1(d). In addition, both frames of Fig. 2 show refraction of the wave, as seen in Fig. 1(b).

Fig. 3 shows several snapshots of the velocity profiles in one of our simulations. As the piston advances, the wave front advances too, at a faster velocity. The piston drive is a step function, but the wave front develops a characteristic width, which is related to the gradient in kinetic energy (velocity) observed in Fig. 2. As a working definition of width, we take the distance between the edge of the front and the point where the velocity is 95% U_p, as shown in Fig. 3. The profile in Fig. 3 has been averaged perpendicularly to the propagation direction over about 10 grains. However, we can identify the width of the wave along the shock direction with the width of the fluctuations normal to the direction of propagation. Close inspection of simulation snapshots, like those in fig. 2 shows that this identification is roughly valid.

Fig. 4 shows the width, normalized to the grain size, versus pressure and grain size. We have adopted a simple functional form to fit our calculations. For Cu, A_v ~0.25 will depend on pressure only weakly in the interval studied, and it is assumed constant. Assuming a power law behavior with grain size and pressure, the observed width can be fit using the following relationship:

$$\Delta z/d = C\, A_v\, (d/d_o)^{\alpha}\, (P/P_o)^{\beta}. \qquad (3)$$

Setting d_o=10 nm, and P_o=47 GPa, we fit the data to get C~5.4; α~ -1/2 and β~ -3/4. As the shock pressure increases, plasticity also increases, but the overall result is a decrease in the width of the front, as seen in experiments and predicted by viscoplastic models[34]. This leads to a steep increase of the strain rate with pressure, as measured for strong, overdriven shocks. As mentioned before, the $d^{1/2}$ grain size dependence is the same dependence that was recently found in simulations[21] of micro-scale polycrystalline Be which did not include GB effects, indicating that this dependence may be somewhat general, and that the role of GBs may be relatively small for all cases. In fact, we note that dislocation activity does not seem significantly to widen the relatively sharp front inside grains, as seen in Fig. 2.

A continuum-level model has shown that the wave front width actually increases with time[17], i.e. the irregularities in the front are enhanced as the wave traverses more grains. Experimental data, however, remains scarce and gives only marginal effects[14,15]. Fig. 5 shows our results, for samples that are ~400 fcc cells (~150 nm) long. After a transient stage, a steady state increase in width is reached, which can be modeled with a power law fit including the number of grains, as:

$$\Delta z/d = C\, A_v\, (d/d_o)^{-1/2}\, (P/P_o)^{-3/4} (N_g/N_{go})^{\gamma}, \qquad (4)$$

with N_{go}~1 for the 20 nm grains, with γ~1/5. The length of our samples may be too small to carry out an appropriate fitting of this dependence. A fit to the continuum model results in ref. (15) gives γ~1/2.

COMPARISON TO WAVE PROPAGATION IN MICRON-SIZED GRAINS

From Figs. 4-5 we are able to obtain a simple analytical form in good agreement with our simulation data. However, given our relatively small simulation data set and the narrow range of grain sizes and pressures accessible to atomistic simulations, it may not be valid to

extrapolate our results to the micro-scale. Chhabildas and Asay[14] have measured an upper limit to the rise time of shocks in Cu targets with d~5 μm at few different pressures. They obtained times of 1.4-2.2 ns, close to their experimental resolution, while our model gives times that are 15-25 times smaller. A worst case-scenario for our model would occur for grain sizes larger than 1 micron at low shock pressure, where the width is expected to be large. Fig. 6 shows experimental data for the elastic wave in such a case. Calculations from a numerical model by M. Meyers[18], which only includes anisotropies as in Fig. 1(b), without GB effects, are also shown. Extrapolation of our simulation data to the experimental conditions for a Ni disk of ~19 mm[13] is shown in Fig. 6, using A_v~0.17 for Ni in Eq. (4), and $t_{rise}=\Delta z/U_s$. We obtain results that are lower by a factor of ~3 than the experimental results and the continuum-level model. That our results are of the same order could be considered somewhat fortuitous, given the simple functional form we use, the extrapolation from nano to micro-scale, and the change of material from Cu to Ni. However, the fact that the continuum model has the same behavior with grain size is likely indicating that the same basic governing principles are at play here. Since that model only considers the first term in Eq. (1), i.e. the anisotropy in the velocity of propagation of the wave for different grains, we suggest that this term dominates the development of the width of the wave front. In our simulations, this seems to be the case even for nanostructured materials, where one would expect the other two terms in Eq. (1) to contribute relatively more than in micron-sized materials. On the other hand, Cu has a particularly high anisotropy factor, which could mask the role of the grain boundary-related terms in developing the width of the front.

Our results may be relevant to the design of NIF targets using micron-sized grains. Since anisotropy dominates the extent of the shock width, using targets with preferential texture,

such as the candidate Be targets[21] (A_v~0.1), would significantly reduce fluctuations at the shock front. The same effect would be achieved using a target with a polycrystalline material having small sound velocity anisotropies, as in the case of polycrystalline carbon (A_v~0)[35]. Future simulations of wave propagation in nanocrystals with hcp and diamond crystalline structures, and with different values of the anisotropy parameter, are needed to asses the range of applicability of our findings which use fcc Cu nanocrystals. Furthermore, a new generation of interferometry techniques[15,36,37] will allow for improved measurements of shock width, including the possible role of fluctuations[36].

SUMMARY

We have presented atomistic simulations of shock wave propagation in nanocrystals. The width of the wave is a function of grain size, pressure, and time. Simple analytical fits show the same scaling with grain size as models not including GB effects[21], i.e. as $d^{1/2}$. In addition, extrapolation to micro-scale experiments[13] and models[18] shows reasonable agreement. Our simulations suggest that the effect of GB in the width of the wave front is small compared to the effect of anisotropy from crystal to crystal. As a result, continuum level models of wave propagation could provide front widths not significantly different from those in more computationally expensive atomistic simulations. Additional MD simulations in nanomaterials are needed to establish the soundness of our hypothesis, including materials with low anisotropy. These simulations would allow more accurate power-law fits and possibly a better understanding of the origin of the exponents governing shock width. Finally, despite all the limitations of atomistic simulations, our results clearly show that nanocrystalline NIF targets would guarantee small fluctuations in the shock front, decreasing the probability for unwelcome instabilities[12].

Authors would like to thank Alex Hamza for fruitful discussions. The work at LLNL was performed under the auspices of the U.S. Department of Energy by University of California, Lawrence Livermore National Laboratory under contract No. W-7405-Eng-48, LDRD 04-ERD-021.

REFERENCES

1. J. R. Weertman, in *Nanostructured Materials: Processing Properties and Potential Applications*, C.C. Koch, Ed. (William Andrew, Norwich, NY, 2001).

2. J. Schiøtz and K.W. Jacobsen, Science **301**, 1357 (2003).

3. H. Van Swygenhoven, M. Spaczer, A. Caro, and D. Farkas. Phys. Rev. **B 60**, 22 (1999).

4. V. Yamakov *et al*., Nature Materials **1**, 1 (2002).

5. M.A. Meyers and K.K. Chawla, *Mechanical Behavior of Materials*, Prentice Hall, (1998).

6. R.A. Lebensohn and C.N. Tome´, Acta Metall. Mater. **41**, 2611 (1993).

7. H.H. Fu, D.J. Benson and M.A. Meyers, Acta Mater. **52**, 4413 (2004).

8. B. Jiang and G.J. Weng, J. Mech. Phys. Solids **52**, 25 (2004).

9. A.C. Lund and C.A. Schuh, Acta Mater. 53, 3193 (2005).

10. B. Remington *et. al*., Met. Mat. Trans. A **35**, 2587 (2004).

11. T.R. Dittrich *et al*., Laser and Particle Beams **17**, 217 (1999).

12. J.D. Colvin *et al*., J. Appl. Phys. **93**, 5287 (2003).

13. O.E. Jones and J.R. Holland, Acta Metall. **16**, 1037 (1968).

14. L. Chhabildas and J. Asay, J. Appl. Phys. **50**, 2749 (1979).

15. K.T. Gagahan *et al*., Phys. Rev. Lett. **85**, 3205 (2000).

16. N.K. Bourne *et al*., Proc. Royal Soc. London A **446**, 309 (1994).

17. M.A. Meyers and M.S. Carvalho, Mat. Sci Eng. **24**, 131 (1976).

18. M.A. Meyers, Mat. Sci Eng. **30**, 99 (1977).

19. D.J. Benson, Wave Motion **21**, 85 (1995).

20. K. Yano and Y. Horie, Phys. Rev. **B 59**, 13672 (1999).

21. R.C. Cook, *Fusion Sci. Technol.* **41**, 155 (2002).

22. J.D. Clayton, J. Mech. Phys. Sol., (2004).

23. Z. Zhao, R. Radovitzky, and A. Cuitino, Acta Mater. **52**, 5791 (2004).

24. E. M. Bringa *et al*., J. Appl. Phys. **96**, 3793 (2004).

25. D.S. Ivanov et al., *Shock Compression of Condensed Matter-2003*, M.D. Furnish, Y.M. Gupta and J.W. Forbes, eds., APS, New York, 2004, p. 225-228.

26. P.K. Schelling, S.R. Phillpot, P. Keblinski, J. Appl. Phys. **95**, 6082 (2004).

27. MDCASK: http://www.llnl.gov/asci/purple/benchmarks/limited/mdcask/

28. Y. Mishin, M. J. Mehl, D. A. Papaconstantopoulos, A. F. Voter, and J. D. Kress, Phys. Rev. B **63**, 224106 (2001).

29. C. L. Kelchner, S. J. Plimpton, and J. C. Hamilton, Phys. Rev. B **58**, 11085 (1998).

30. L. Holian and P.S. Lomdahl, Science **280**, 2085 (1998).

31. K. Kadau, T.C. Germann, P.S. Lomdahl, and B.L. Holian, Science **296**, 1681 (2002).

32. F. A. Sapozhnikov, V.V. Dremov and M.S. Smirnova, J. Phys. IV France **110**, 323 (2003).

33. E.M. Bringa *et al*., submitted to Science (2005).

34. A. Molinari and G. Ravichandran, J. Appl. Phys. **95**, 1718 (2004).

35. J.K. Krüger *et al*., Diamond and Related Mat. **9**, 123 (2000).

36. Yu. I. Mescheryakov, N. A. Mahutov, and S. A. Atroshenko, J. Mech. Phys. Solids **42**, 1435 (1994).

37. M. Hauer *et al*., Thin. Sol. Films **453**, 584 (2004).

Figure Captions

FIG. 1. Schematic of wave propagation in a polycrystal. The dotted line indicates the wave front. (a) single crystal.(b)-(d) polycrystals showing: (b) anisotropy due to different crystalline orientations, (c) GB acting as scattering centers, and (d) GB enhancing plasticity induced by the wave front.

FIG. 2. Snapshots of our MD simulation that show the wave front at two different times. Grain boundary atoms are overlapped as small black dots. d=5 nm, P=22 GPa, U_p=0.5 km/s and 10% strain. Atoms are colored according to their kinetic energy (red, high –moving at U_p; blue, low –unshocked). The upper frame shows a sharp front inside the grains, with some refraction due to orientation. Note that the energy levels track the GB, and that in frame (b) the front itself tracks the shape of one of the grains. Some of the stacking faults generated by the wave are marked with blue circles.

FIG. 3. Three snapshots from an MD simulation for d=20 nm and P=47 GPa showing velocity profiles, averaged in slices one lattice parameter, a_0, thick, perpendicular to the shock propagation direction. The measurement of the width Δz at t=12 ps is indicated.

FIG. 4. Front width, normalized to the grain size, versus grain size and pressure. Solid lines show the fitting from Eq. (3). Width was measured when the wave front had traveled ~70 nm.

FIG. 5. Evolution of the width with scaled time, for two simulated cases showing the power law evolution that gives γ=1/5.

FIG. 6. Experimental results[13] compared to the continuum level model by Meyers[18], and the extrapolation of our MD results using Eq. (4).

Figures

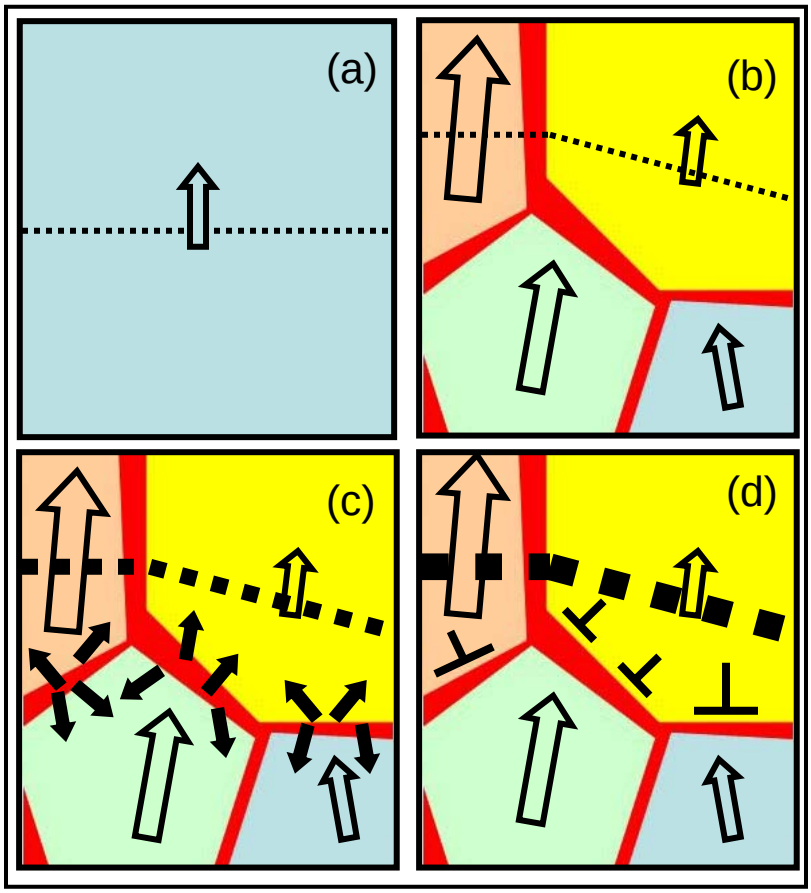

FIGURE 1

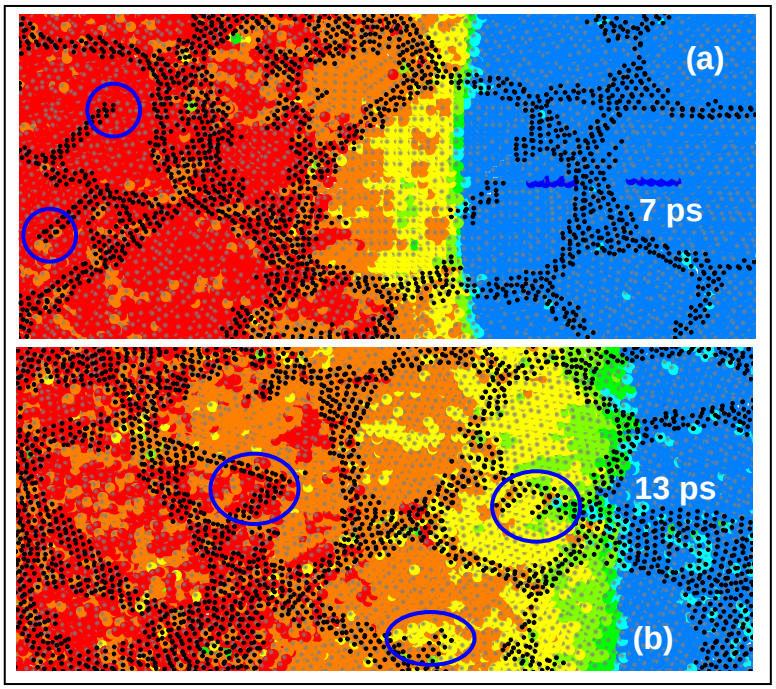

FIGURE 2

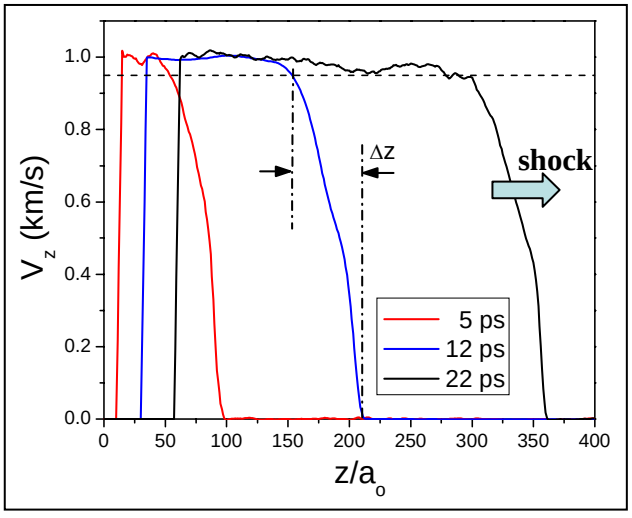

FIGURE 3

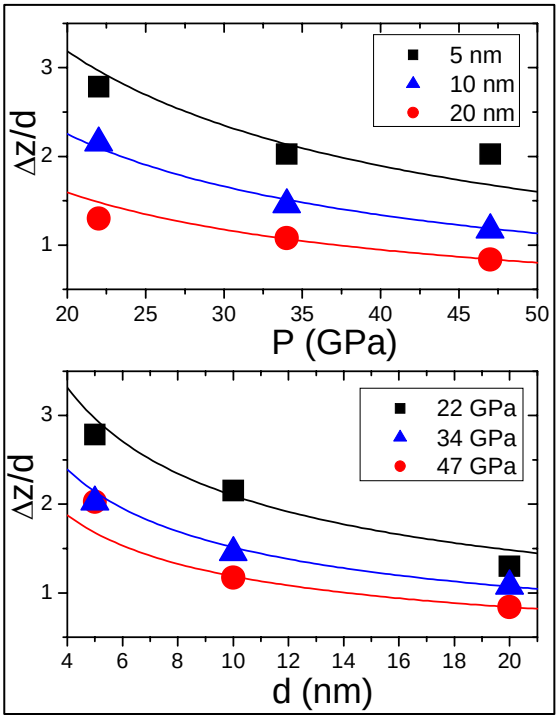

FIGURE 4

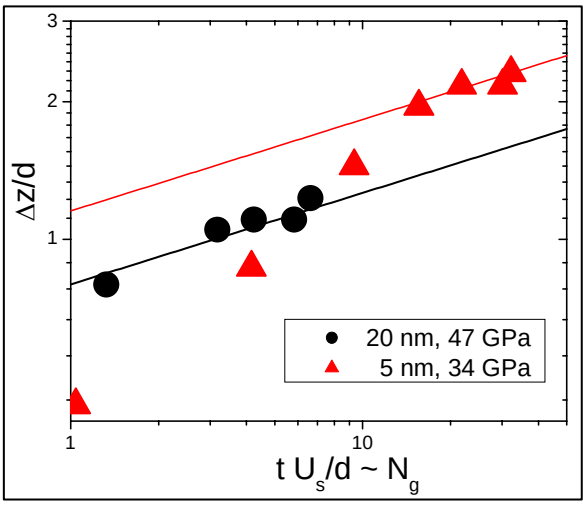

FIGURE 5

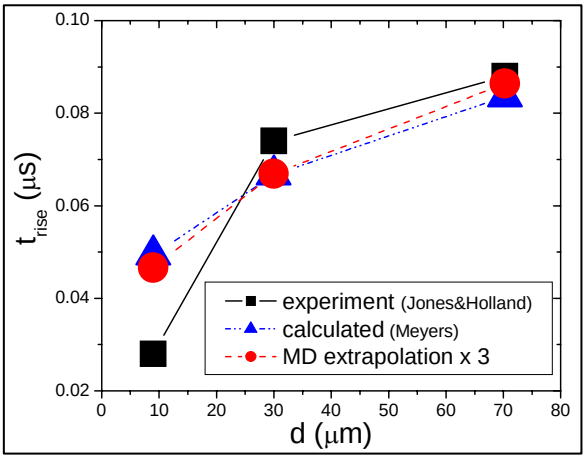
0.10
0.08
0.06
0.04
0.02
t_{rise} (μs)
0
10
20
30
40
50
60
70
80
d (μm)
experiment (Jones&Holland)
calculated (Meyers)
MD extrapolation x 3

FIGURE 6